UNCLASSIFIED

Defense Technical Information Center
Compilation Part Notice

ADP020038

TITLE: Microcavitation and Spot Size Dependence for Damage of Artifically Pigmented in hTERT-RPE1 Cells

DISTRIBUTION: Approved for public release, distribution unlimited

This paper is part of the following report:

TITLE: Laser Interaction with Tissue and Cells XV. Held in San Jose, Ca on 26-28 January 2004.

To order the complete compilation report, use: ADA436676

The component part is provided here to allow users access to individually authored sections of proceedings, annals, symposia, etc. However, the component should be considered within the context of the overall compilation report and not as a stand-alone technical report.

The following component part numbers comprise the compilation report:
ADP020007 thru ADP020056

UNCLASSIFIED

Microcavitation and spot size dependence for damage of artificially pigmented hTERT-RPE1 cells[‡]

Brian M. Mills[a], Tracie M. Connor[a], Michael S. Foltz[b], Jacob Stolarski[a], Kristy L. Hayes[a], Michael L. Denton[b], Debbie M. Eikum[b], Gary D. Noojin[b], and Benjamin A. Rockwell[a]

[a]Air Force Research Laboratory, AFRL/HEDO, Brooks Air Force Base, TX, 78235-5214
[b]Northrop Grumman Information Technology, San Antonio, TX, 78228-1330

ABSTRACT

We performed measurements to validate damage threshold trends in minimum visible lesion (MVL) studies as a function of spot size for nanosecond laser pulses. At threshold levels, nanosecond pulses produce microcavitation bubbles that expand and collapse around individual melanosomes. This microcavitation process damages the membranes of retinal pigment epithelium (RPE) cells. A spot size study on retinal explants[1] found cell damage fluence (energy/area) thresholds were independent of spot size when microcavitation caused the damage, contradicting past *in vivo* retinal spot size experiments.[2 3 4] The explant study (*ex vivo*) used a top-hat beam profile, whereas the *in vivo* studies used Gaussian beams. The difference in spot size trends for damage *in vivo* versus *ex vivo* may be attributed to the optics of the eye but this has not been validated. In this study, we exposed artificially pigmented human RPE cells (hTERT-RPE1)—*in vitro*—to 7 ns pulsed irradiation from a Ti:Sa TSA-02 regenerative amplifier (1055 nm) with beam diameters of 44, 86, and 273 μm (Gaussian beam profiles). We detected the microcavitation event with strobe illumination and time-resolved imaging. We used the fluorescent indicator dye calcein-AM, with excitation by an Argon laser (488 nm), to assess cell damage. Our current results follow trends found in the *in vivo* studies.

Keywords: Microcavitation, spot size, retinal, fluorescence microscopy, RPE cell culture

1. INTRODUCTION

The interaction between laser radiation and light-absorbing microparticles in the eye is a significant laser eye safety concern due to the widespread use and availability of lasers emitting radiation in the retinal hazard regime. Melanosomes (melanin-containing organelles found in RPE cells) readily absorb near-infrared radiation.[5] They absorb pulsed laser energy and release this energy as heat, thus vaporizing the surrounding fluid. This process generates temporary vapor bubbles (microcavitation) around the melanosomes.[6] When these microcavitation bubbles expand and collapse, they breach the cell membrane and destroy the cell.[7] RPE cell damage by microcavitation precedes cell damage by other thermal methods when the irradiation is delivered in single pulses less than 3 μs in duration.[8]

Roegener and Lin identified intracellular microcavitation as the damage mechanism for RPE cells when exposed to pulsed radiation in the visible spectrum.[1] Their study used RPE explants from calf eyes (*ex vivo*) and exposed them to 532 nm laser irradiation pulsed at 100 ps with a top hat beam profile. They irradiated the RPE cells at various spot sizes and found the fluence required to cause cellular release of calcein dye 50% of the time (ED_{50}) to be nearly constant at 0.043 J/cm^2 for all spot sizes—20, 40, 100, and 200 μm. Their results contradict *in vivo* minimum visible lesion (MVL) threshold studies, which show the fluence required for cell damage decreases as spot size increases.[2 3 4] Here we investigate the dependence of cell damage fluence threshold on spot size for RPE

[‡] Opinions, interpretations, conclusions, and recommendations are those of the authors and are not necessarily endorsed by the United States Air Force.

Laser Interaction with Tissue and Cells XV, edited by
Steven L. Jacques, William P. Roach, Proc. of SPIE Vol. 5319
(SPIE, Bellingham, WA, 2004) · 1605-7422/04/$15 · doi: 10.1117/12.530331

cells *in vitro*. We hypothesize microcavitation will breach the hTERT-RPE1 cell membranes at a fluence threshold constant for all spot sizes.

2. MATERIALS AND METHODS

2.1 CELL PREPARATION:

We grew cell cultures at 37°C in a 5% CO_2 atmosphere. We maintained stock cultures of the human RPE cell line hTERT-RPE1 (ClonTech) in DMEM/F12 medium supplemented with 10% fetal bovine serum (FBS; Atlanta Biochemicals). At 2-4 days prior to exposure, we plated the cells into 48-well microtiter dishes at a density of approximately 75,000 (cells/cm^2). We obtained artificially pigmented hTERT-RPE1 cultures as previously described.[9]

Prior to laser exposures, we added 100 µl of 1.7 µM calcein-AM (Molecular Probes, Portland, OR, cat# C-3099) in HBSS buffer to the cells. We then incubated the cells for 10 min at 37°C and carefully rinsed them with 1 ml HBSS. Viable cells took up the dye internally, and converted the calcein-AM to calcein via cellular esterase enzymes. Calcein was unable to diffuse out of the cell as long as the cell maintained the integrity of its cellular membrane. This allowed us to assess real-time cell viability (cell membrane integrity) during the laser exposure experiments. During exposure, each well in the microtiter dish contained 100 µl HBSS.

2.2 EXPERIMENT SET-UP:

In order to observe the targeted cells before, during, and after exposure, we set up a microscope containing three beam paths (see Figure 1): (1) the irradiation beam, (2) the illumination beam, and (3) the fluorescence excitation beam.

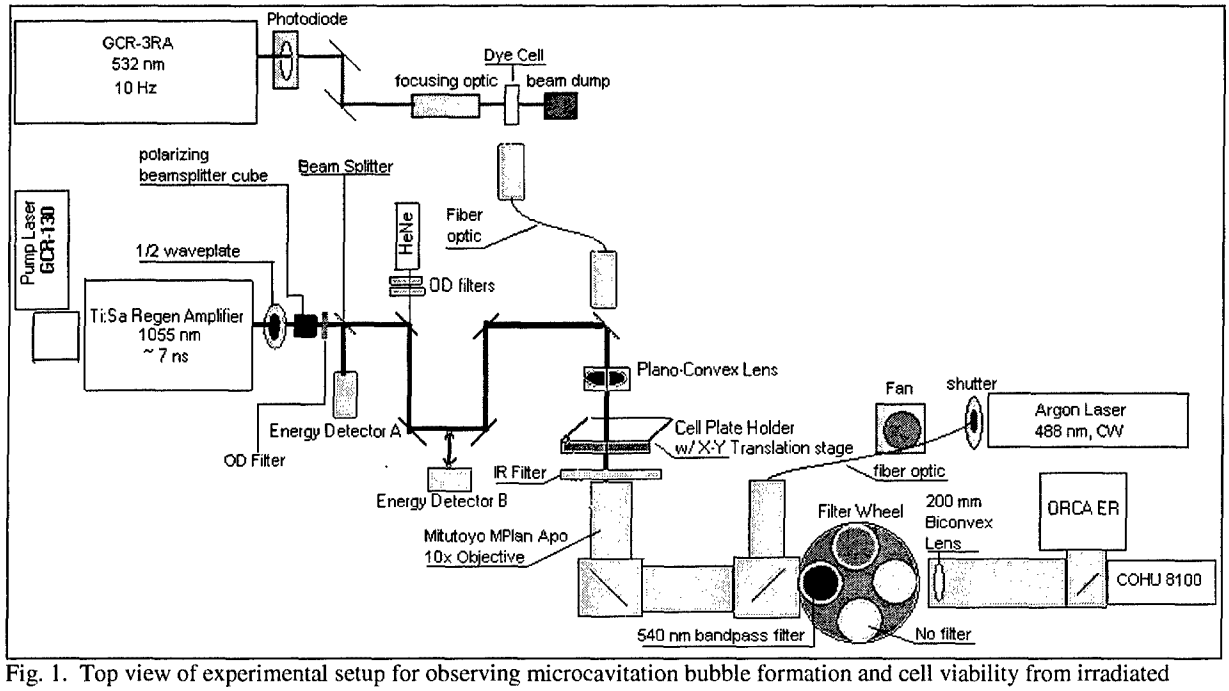

Fig. 1. Top view of experimental setup for observing microcavitation bubble formation and cell viability from irradiated hTERT-RPE1 cells.

The irradiation beam consisted of a Spectra Physics Q-switched, frequency doubled, Nd:YAG GCR-130 laser operating at 10Hz. This laser pumped a Ti:Sapphire regenerative amplifier. The regenerative amplifier generated a 7 ns, 1055 nm, Gaussian pulse and provided the wide range of energies required for our spot sizes. We

controlled the pulsed energy to the sample with a half-waveplate, polarizing beam-splitter cube and a neutral density filter. A beam splitter directed a portion of the beam into a reference detector (Detector A). The remaining energy passed through the splitter and hit the second energy detector (Detector B) in front of the sample. We measured and recorded the beam splitter ratio (B/A) before every experimental run. The beam then traveled through a series of mirrors, a periscope, and a plano-convex lens positioned appropriately to focus the beam to the desired spot size on the sample. After each shot, we recorded the pulse energy from Detector A and multiplied by the B/A ratio to determine the energy delivered to the sample. We used fast photodiodes and an oscilloscope to verify the pulse width of the regenerative amplifier and monitor the time delay between the strobe pulse and the irradiation exposure. A computer, programmed using LabVIEW, automated all data collection.

The illumination beam consisted of a Spectra Physics Model GCR-3RA Nd:YAG regenerative amplifier running in the nanosecond mode. We frequency-doubled the output to 532 nm and ran it at 10 Hz. We focused the energy from the GCR-3RA on a dye cell containing Rhodamine 640 dissolved in methanol. The dye absorbed the 532 nm energy and emitted ~580 nm. We coupled the ~580nm scatter into a large core fiber at 90 degrees to the pump beam. We positioned the fiber output directly above one of the IR mirrors that turned the irradiation beam to the sample and gave our illumination beam the same path into the sample as the irradiation beam. Two delay generators allowed time-resolved imagery: one controlling the delay between the irradiation beam and the illumination beam; the other triggered the regenerative amplifier to output a single pulse and triggered the Hamamatsu ORCA ER camera to capture an image. The LabVIEW software controlled the imaging sequence, one strobe within a second before irradiation, a second strobe 500 ns after irradiation, and a final strobe less than a second hence. We captured each illuminated image of our sample with the ORCA ER camera and saved the digitized images to computer.

The fluorescence excitation beam consisted of a Spectra Physics Argon Laser Model 262A emitting 488 nm, continuous wave energy. We coupled the energy into a large core, multi-mode fiber. To reduce the coherence of this light, we dithered the fiber with a fan which scrambled the mode in the fiber and reduced the coherence induced speckle in our images. We blocked the 488 nm energy with a shutter that we manually opened when needed. Two fluorescence images were taken, one before irradiation and one after irradiation. These images showed the fluoresced culture areas surrounding our laser exposure sites. During fluorescence image acquisition, we used a bandpass filter to pass the green cellular fluorescence to the ORCA ER camera while blocking the 488 nm and 580 nm beams.

2.3 PROCESS FOR IDENTIFYING MICROCAVITATION AND CELL BREACH:

We irradiated cells at three different (44, 86, and 273 μm diameter) spot sizes. With each change in spot size, we changed the focusing lens and moved it the appropriate distance from the sample. By placing our microtiter dish of hTERT-RPE1 cells in a custom plate holder and attaching it to a stage controller capable of micrometer movement in three dimensions (controlled by LabVIEW software), we were typically able to expose sixteen different locations within each well. We fixed the 10x optical objective of our vertical microscope under the microtiter dish. By adjusting the distance between the microscope objective and the CCD camera, we set the magnification of our microscope at 10x for each spot size—giving us approximately 1 μm resolution. Each experimental run generally consisted of exposing two wells followed by data collection and analysis.

After positioning the microtiter culture dish, we located and focused our target cells. First, we placed the stage in its proper vertical position by focusing a real-time image of our target cells, illuminated by our 10 Hz strobe beam and displayed on a television monitor attached to a COHU CCD camera. To assure we had an exact focus, we inserted the band-pass filter, opened the shutter blocking the fluorescence excitation beam, and quickly examined a real-time fluorescence image from the COHU camera and made minor adjustments as necessary. This also gave us a good picture of our cells—we could check for any discrepancies and move to the next spot if necessary.

Once properly focused, we captured a fluorescence image (before-irradiation) of our target cells. If cells were viable (i.e. their cellular membranes were intact), then the previously loaded calcein dye would fluoresce green upon excitation by the 488 nm argon laser (see Figure 2-A). The LabVIEW software took care of the next four processes. First, it captured an illumination image of the cells (see Figure 2-C). Then, it triggered the irradiation

beam—a 7 ns pulse. Next, it captured an illumination image of the cell 500 ns after irradiation to witness any microcavitation bubbles (see Figure 2-D). Then, it captured a final illumination image (see Figure 2-E) within a second after irradiation. Next, we inserted the bandpass filter and opened the shutter exposing the cells to 488 nm light one last time to capture the final fluorescence image (after-irradiation). If the fluence of our irradiation beam was high enough to cause microcavitation—damaging the cell's membrane and diffusing the calcein from the cell—then that cell would no longer show fluorescence and show up as a dark spot on this image (see Figure 2-B). If the fluence of our irradiation beam was below the threshold for microcavitation, then this image would appear similar to the before-irradiation image (see Figure 2-A).

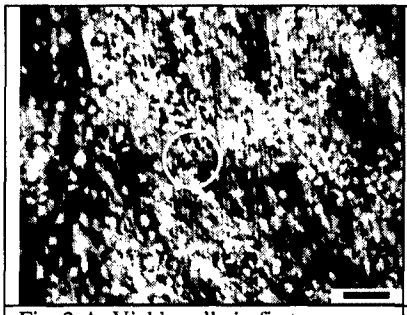

Fig. 2-A: Viable cells in first fluorescence image.

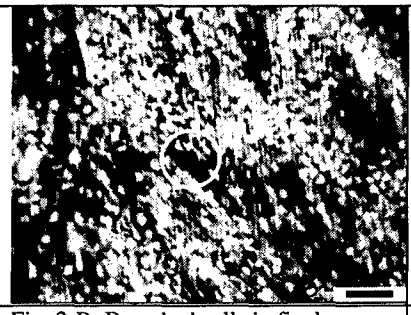

Fig. 2-B: Breached cells in final fluorescence image.

Fig. 2-C: Illumination image of cells—within a second prior to irradiation.

Fig. 2-D: Illumination image of microcavitation bubble 500 ns after irradiation from 44μm diameter beam.

Fig. 2-E: Illumination image of cells within a second after irradiation.

Fig.- 2. Actual data from the 44μm diameter spot size irradiation beam. The white circle highlights the events (cell breach and microcavitation). The black bar in the lower right corner represents 100μm.

2.4 FLUENCE THRESHOLD ANALYSIS:

The standard technique for ascribing a threshold value is by empirically establishing that energy level which will produce damage in the target 50% of the time (commonly known as the ED_{50} level).[10] We used the Probit procedure[11 12] to estimate the ED_{50} fluence required to damage our cells for each spot size and the ED_{50} fluence required to witness a microcavitation bubble. This procedure also gave us estimates for the 95 percent confidence intervals for our ED_{50} values. When we exposed the cells and failed to witness any change between the before-irradiation fluorescence image and the after-irradiation fluorescence image, we recorded that data point as a zero. Conversely, when we exposed the cells and witnessed a dark spot in the after-irradiation fluorescence image (where microcavitation occurred), we recorded that data point as a one. We used the same procedure for microcavitation bubble thresholds—if we saw no bubble in our illumination image, then we recorded that data point as a zero; if we saw a bubble, then we recorded that data point as a one.

3. RESULTS AND DISCUSSION

Our *in vitro* investigations followed the trend set by previous *in vivo* experiments showing ED_{50} fluence thresholds dependent on spot size; namely, ED_{50} thresholds decreased as spot size diameters increased. Our results are summarized graphically in Figure 3-A and compared with similar *in vivo* studies and the Roegener/Lin *ex vivo* study in Figure 3-B.

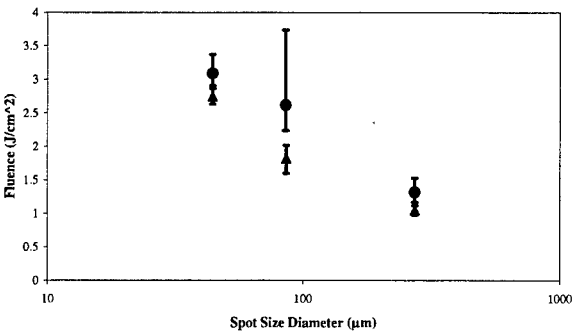

Fig. 3-A. Plot of cell breach fluence thresholds and microcavitation bubble thresholds vs. irradiation spot size diameters from our experiment. The triangles represent our fluence ED_{50} threshold results and the circles represent our microcavitation bubble ED_{50} threshold results—the dashes above and below our data points define the estimated 95% confidence intervals about our ED_{50} estimates.

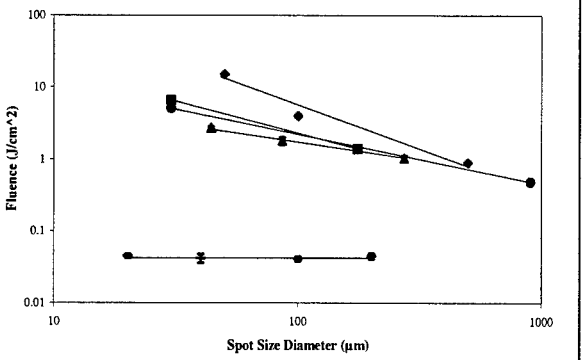

Fig. 3-B. Logarithmic plots of cell breach fluence thresholds vs. irradiation spot size diameters. The triangles represent our study. The diamonds represent the Beatrice *et al* study.[2] The squares represent the Borland *et al* study.[3] The circles represent the Griess *et al* study.[4] The dashes represent the Roegener/Lin study.[1] The straight lines are shown for visual aid only.

We expected the microcavitation bubble ED_{50} thresholds to overlap the damage fluence ED_{50} thresholds—previous studies show microcavitation is a mechanism of cell damage.[5] Our results in Figure 3-A show membrane breach occurred before microcavitation; in fact, the 95% confidence intervals fail to overlap for each spot size indicating the two events were significantly different. We believe, in all cases, microcavitation damaged the membranes of our artificially pigmented hTER-RPE1 cells; however, we were unable to witness this microscopic event. Lin and Kelly observed the typical lifetime of a microcavitation bubble around an individual melanosome (produced at threshold energy) to extend from 1 ns to a few 100 ns after irradiation—disappearing after it collapses.[5] This suggests if we illuminated our cells at any time beyond a few 100 ns after the irradiation pulse at threshold energy, then we missed capturing the event. Lin and Kelly observed cells exposed to above-threshold energy levels generated multiple microcavitation bubbles from multiple melanosomes which then coalesced and formed larger bubbles with longer lifetimes.[5] They found the coalesced bubble lifetimes were 580 ns at 1.4x threshold and 850 ns at 2.2x threshold.[5] Our illumination timing, set 500 ns after pulse irradiation, was sufficient to capture coalesced bubbles absorbing energies above cell breach threshold levels (1.3x, on average) but too late to capture the individual melanosome microcavitation bubbles before they collapsed and disappeared. In a different study, Lin *et al*, showed bubble diameters around individual melanosomes at maximum expansion were a few micrometers, while coalesced bubbles filled the cells (up to 20µm in diameter).[7] Our ~1µm resolution was sufficient to witness coalesced microcavitation but perhaps not enough to observe microcavitation bubbles around individual melanosomes. We will investigate this further in future experiments.

The studies we displayed in Figure 3-B were run with parameters similar to our study. The three *in vivo* studies used irradiation beams near 1060 nm with pulse durations near 15 ns and Gaussian profiles.[2] [3] [4] The Roegener/Lin *ex vivo* study used an irradiation beam at 532 nm, 100 ps, and had a top-hat beam profile.[1] We expected the Roegener/Lin study data to fall well below our data on the logarithmic plot as infrared laser exposures have a higher damage threshold than their visible counterparts due to reduced melanin absorption at the longer wavelengths. [13] In addition, longer pulse durations have a higher damage threshold than shorter pulses. Roegener and Lin used an irradiation beam half our wavelength with a pulse duration 70x shorter than ours.

Thus, we were not as concerned with the location of our data on the graph as we were in its trend relative the Roegener/Lin study. Our data clearly followed the trend from existing *in vivo* data, where cellular damage fluence threshold decreased as spot size increased. This fails to support both our experiment hypothesis and the results from the Roegener/Lin study—constant cellular damage thresholds for all spot sizes. We are examining our experimental uncertainty to evaluate their values for our parameter set, but initial evaluation shows these to not overcome the differences measured. Possible uncertainties and limitations include: energy detection, spot size measurement, and minimum event-detectability (a function of microscope resolution as well as fluorescence and bubble detection). We are determining the impact of these parameters on our results.

4. CONCLUSIONS

We measured the fluence required for RPE cell damage as a function of spot size using a Gaussian beam profile. The pulse duration was 7 ns at a wavelength of 1055 nm. We have shown that the fluence required for RPE damage changes as a function of spot size, contrary to previous measurements using a flat top beam. We are investigating the mechanisms responsible for this result.

5. ACKNOWLEDGEMENTS

This research reported herein was supported by the Air Force Office of Scientific Research (92HE04COR), The Air Force Research Laboratory, Human Effectiveness Directorate, Directed Energy Bioeffects Division, Optical Radiation Branch (7757B206), and Contract: F33615-92-0017.

REFERENCES

[1] Roegener, Jan and Lin, Charles P., "Photomechanical effects—experimental studies of pigment granule absorption, cavitation, and call damage," *Proc SPIE*, vol. 3902, pp. 35-40, 2000.

[2] Beatrice, Edwin S. and Shawaluk, Paul D., *Q-Switched Neodymium Laser Retinal Damage in Rhesus Monkey*, Joint AMRDC-AMC Laser Safety Team Memorandum Report M73-9-1, 1973.

[3] Borland, R.G., Brennan, D.H., Marshall, J., and Viveash, J.P., "The Role of Fluorescein Angiography in the Detection of Laser-induced Damage to the Retina: A Threshold Study for Q-switched, Neodymium and Ruby Lasers," Experimental Eye Research **27**: 471, 1978.

[4] Griess, Gary A. and Blankenstein, Michael F., "Ocular Damage from Multiple-pulse Laser Exposures," Health Physics **39**: 921-927, 1980.

[5] Lin, Charles P. and Kelly, Michael W., "Cavitation and acoustic emission around laser-heated microparticles," Appl. Phys. Lett. **72**(22): 2800-2802, 1998.

[6] Leszczynski, D., Pitsillides, C.M., Pastilla, R.K., Anderson, R.R., and Lin, C.P., "Laser-beam-triggered Microcavitation: A Novel Method for Selective Cell Destruction," Radiation Research **156**: 399-407, 2001.

[7] Lin, C.P., Kelly, M.W., Sibayan, S.A.B., Latina, M.A., and Anderson, R.R., "Selective Cell Killing by Microparticle Absorption of Pulsed Laser Radiation," IEEE Journal of Selected Topics in Quantum Electronics, **5**(4): 963-968, 1999.

[8] Brinkmann, R., Huettmann, G., Roegener, J., Roider, J., Birngruber, R., Lin, C.P., "Origin of Retinal Pigment Epithelium Call Damage by Pulsed Laser Irradiance in the Nanosecond to Microsecond Time Regimen," Lasers in Surgery and Medicine, **27**: 451-464, 2000.

[9] Denton, M.L., Eikum, D.M., Noojin, G.D., Storlarski, D.J., Thomas, R.J., Glickman, R.D., and Rockwell, B.A., "Pigmentation in NIR Laser Tissue Damage," *Proc SPIE*, vol. 4953, pp. 78-84, 2003.

[10] Payne, D.J., Jost, T.R., Elliott, J.J., Eilert, B.G., Lott, L., Lott, K., Noojin, G.D., Hopkins, R.A. Jr., Lin, C.P., and Rockwell, B.A., "Cavitation thresholds in the rabbit retina pigmented epithelium," *Proc SPIE*, vol. 3601, pp. 27-31, 1999.

[11] Cain, C.P. and Noojin, G.D., *AL/OE-TR-1996-0102 A Comparison of Various Probit Methods for Analyzing Yes/No Data on a Log Scale*, Brooks AFB, TX, USAF Armstrong Laboratory: 46, 1996.

[12] Finney, D.J., Probit Analysis, 3rd ed., New York, NY, Cambridge University Press, 1971.

[13] Cain, C.P., Noojin, G.D., Storlarski, D.J., Thomas, R.J., and Rockwell, B.A., *AFRL-HE-BR-TR-2003-0029 Near-infrared Ultrashort Pulse Laser Bioeffects Studies—Final Report*, Brooks AFB, TX, USAF Research Laboratory: 25, 2003.